Popular Summary

Symmetric Resonance Charge exchange cross section based on Impact parameter treatment

Kazem Omidvar
Data Assimilation Office, NASA/Goddard Space Flight Center, Greenbelt, MD 20771

Kendrah Murphy
Physics Department, Skidmore College, Saratoga Spring, New York 12866

Journal: The Journal of Chemical Physics

A key reaction for the transfer of the solar energy to the thermosphere layer of the atmosphere is charge exchange between singly ionized oxygen atom and the atomic oxygen. In this way the energetic ionized oxygen atoms, which have been produced and energized through photoionization of oxygen atoms by the solar radiation, become energetic neutral atomic oxygen, heating the thermosphere.

The cross section for this reaction is not known accurately, and there is a discrepancy of 20% or more between theory and experimental observations. In this paper we have developed a new method for calculating the cross section.

The work consists in evaluation of a number of double integrals that are difficult to evaluate analytically, but we have evaluated numerically. Results of calculations are compared with measured cross sections. Good agreement have been obtained with the results of laboratory measurements for the ion-atom pairs H^+-H, He^+-He, and Ar^+-Ar. The method is mostly suited for hydrogenic and closed shell atoms. Results obtained for O^+-O charge exchange do not compare favorably with measurements. Improvement of the model is planned for the future. Some erroneous approximations in the literature by other authors have been corrected.

SYMMETRIC RESONANCE CHARGE EXCHANGE CROSS SECTION BASED ON IMPACT PARAMETER TREATMENT

Kazem Omidvar
Data Assimilation Office, NASA/Goddard Space Flight Center, Greenbelt, MD 20771

Kendrah Murphy
Physics Department, Skidmore College, Saratoga Springs, New York 12866

Abstract. Using a two-state impact parameter approximation, a calculation has been carried out to obtain symmetric resonance charge transfer cross sections between nine ions and their parent atoms or molecules. Calculation is based on a two-dimensional numerical integration. The method is mostly suited for hydrogenic and some closed shell atoms. Good agreement has been obtained with the results of laboratory measurements for the ion-atom pairs H^+-H, He^+-He, and Ar^+-Ar. Several approximations in a similar published calculation have been eliminated.

1.INTRODUCTION

To study the symmetric resonance charge exchange cross sections, we apply in this paper a two-state hydrogenic approximations and the impact parameter treatment to obtain intermediate energy range cross sections. Calculation is similar to a calculation made by Rapp and Francis[1]. However, due to basically lack of fast computers, these authors in an attempt to solve the problem analytically, have made a number of questionable approximations. As a result, their results fall generally below measured cross sections, and other more accurate calculational cross sections. In this paper, these approximations have been eliminated, resulting in more accurate calculations, and better agreement with measurements. The advantage of the method is its simplicity. Although the method is based on the energy difference between quantum mechanical symmetric and anti symmetric states of the molecular ion formed by the parent atom and ion, the cross

section depends only on the ionization potential of the target atom, and no knowledge of the molecular ion wave function is necessary. Except at very low energies, for hydrogenic and some closed shell atoms, the method gives surprisingly good results in agreement with measurements, and comparable to full quantum mechanical results.

2. THEORY AND CALCULATION

The resonant charge transfer between a hydrogen atom nucleus and the ground state hydrogen atom is given by the reaction

$$H_B^+ + H_A \rightarrow H_B + H_A^+. \qquad (1)$$

Since the initial and final states of (1) have the same energies, the two states of the system are degenerate. When the two particles in (1) are far apart, the interaction between the two particles is weak, and the wave function of the system can be represented as the product of one particle wave functions. However, as the two particles approach each other, the inter nuclear and electron- distant nucleus interactions become strong, and their effect can not be neglected. Since the expectation values of the non-diagonal elements of the Hamiltonian with respect to these interactions are not zero, a diagonalization to obtain the eigenfunctions and eigenvalues has to be performed. As a result we obtain two distinct wave functions, symmetric and anti symmetric with respect to the interchanges of the particles nuclei, each belonging to either the initial or the final states of the reaction (1). The charge transfer then corresponds to a transition between the symmetric and anti symmetric states.

Eigenvalues belonging to the anti symmetric and symmetric cases, called E_a and E_S, are given elsewhere[2,3]. Neglecting values of the overlap integrals of the wave functions for H_A and H_B, the difference between the anti symmetric and symmetric eigenvalues is given by

$$\Delta E(R) = E_a - E_s = \frac{Ze^2}{a_0} e^{-ZR/a_0}(1 + \frac{ZR}{a_0}), \qquad (2)$$

where R is the inter nuclear distance, e and a_0 are the electronic charge and the Bohr radius, and Z is the effective charge of the hydrogenic atom..

Measuring length in units of a_0 , the cross section for the charge transfer in units of πa_0^2 in the impact parameter treatment is given by

$$\sigma(v) = 2\int_0^\infty P(v,b)bdb, \qquad (3)$$

where v is the initial velocity of the projectile, b is the impact parameter, and p(v,b) is the probability of charge transfer for a projectile of velocity v, and impact parameter b. Bates, Massey, and Stewart[4] have shown that this probability is given by

$$P(v,b) = \sin^2\left[\frac{1}{\hbar}\int_b^\infty \frac{\Delta E(R)}{v(R)}\left[1-\frac{v^2b^2}{(Rv(R))^2}\right]^{-1/2} dR\right], \qquad (4)$$

where v(R) is the projectile velocity as a function of R. It has been shown by Jackson5 that, without loss of much accuracy, v(R) can be replaced by its asymptotic value v=v(R>>1).· Then (4) takes the form

$$P(v,b) = \sin^2\left[\frac{1}{\hbar v}\int_b^\infty \frac{R\Delta E(R)}{(R^2-b^2)^{1/2}} dR\right] \qquad (5)$$

In evaluating (5), we introduce cartesian coordinates. We choose the projectile as being along the x-axis, and we choose the x,y coordinates of the target as being 0 and b. Then $R = (x^2+b^2)^{1/2}$. Since most contribution to the cross section arises from large values of R, for practical purposes we neglect 1 in the bracket on the right-hand-side of (2). Making use of the identity $Z^2 = I/I_0$, where I and I_0 are the ionization potentials of the hydrogenic and hydrogen atoms, combination of (2) and (5) results in

$$P(v,b) = \sin^2\left[\frac{Iv_0}{I_0 v a_0^2}\int_0^\infty (x^2+b^2)^{1/2}\exp\left[-\left(\frac{I}{I_0}\right)^{1/2}(x^2+b^2)^{1/2}/a_0\right]dx\right], \qquad (6)$$

where b is the impact parameter in units of the Bohr radius a_0, v is the relative velocity of the two colliding particles, and $v_0 = 2.18769 \times 10^8 \text{cm/s}$ is the Bohr velocity. Introducing

$$g(v,b) = \frac{Iv_0}{a_0^2 I_0 v} \int_0^\infty (x^2 + b^2)^{1/2} \exp\left[-(\frac{I}{I_0})^{1/2} (x^2 + b^2)^{1/2} / a_0 \right] dx, \quad (7)$$

Eq. (3) takes the form

$$\sigma(v) = 2 \int_0^\infty \sin^2(g(b,v)) b db \quad (8)$$

For $v << v_0$, as usually is the case, g(v,b) is much larger than unity, and for b<<1, Eq. (8) shows that the integrand in (8) oscillates rapidly, making the numerical evaluation of the integral in(8) difficult. As is the practice, we introduce a parameter b^*, and for $0 \le b \le b^*$ we replace $\sin^2(g(v,b))$ by its average equal to 1/2. Equation (8) can then be written alternatively as

$$\sigma(v) = \frac{1}{2} b^{*2} + 2 \int_{b^*}^\infty \sin^2(g(v,b)) b db. \quad (9)$$

For each incident velocity, we find a range of b^* for which the value of the integral in (9) for various values of b^* in this range does not change by more than 1%. Eq. (7) shows that as v increases, g(b,v) decreases, and smaller values for the range of b^* is necessary. Combining Eqs (7) and (9), $\sigma(v)$ has been evaluated by a double numerical integration.

The double numerical integration was performed on the calculator MATLAB. For the evaluation of the integral in (7), we replace the upper limit of the integral by 10., the relative error due to this replacement is less than 10^{-4}. We also found, by trial, that it is sufficient to set the upper limit of the integral in (9) equal to 18. For both integrals in (7) and (9) we have used 85 mesh points. Setting the number of mesh points above this value, changed the value of the cross section by less than 1%. In this investigation, values of the cross sections for both 85 and 90 mesh points were determined.

3. RESULTS AND DISCUSSION

Results are presented in one Table and 12 figures that follows. In Table I, as a sample of the method of our computation, hydrogen atom-hydrogen ion charge exchange is considered. Columns 3 and 4 give the range of b^*, and the number of samples taken in this range. Column 5 gives our calculated cross sections with their associated root-mean-squared uncertainties. The sixth and seven columns are cross sectional values of Rapp and Francis[1], and Dalgarno and Yadav[6], repectively.

Before discussion of the figures it should be pointed out that investigators have shown that in intermediate energy range the squared root of the resonance charge exchange cross sections are proportional to the negative of the logarithm of the projectile energy. As a result, it is customary to plot the squared root of the cross section versus the logarithm of the projectile energy, resulting in straight graph lines with negative slopes. We also have followed the same procedure in all figures except one.

As can be seen from Eqs. (3) and (6), for $v_0 / v << 1$, the cross section becomes inversely proportional to the energy. Then, the graphs shown in our figures should deviate from constant slope at high energies. This in fact is the case, and we see in the following figures that the slope of the curves bend and become more positive as energy increases. In addition, at high energies, the curves show some irregular variation in their slopes, which is thought to be due to the change of the regime of the cross section with respect to energy.

Figure 1 shows comparison between our results and the results of Rapp and Francis[1]. Their results fall by about 20% below our results. We believe the discrepancy is due to the approximations made by these authors.

We also compare our results to the total quantum mechanical perturbed stationary states calculations of Dlgarno and Yadav[6], and Hunter and Kuriyan[7]. Calculation of Hunter and Kuriyan is the most uptodate, and is extended to much lower energies than others, where quantum mechanical effects on the cross section is shown. This effect is absent in our calculation. The agreement of the present calculation with those of Dalgarno and Yadav[6], and Hunter and Kurian[7], in the intermediate energy range is quite striking.

The experimental results of Fite et al.[8] are also shown in the figure with some earlier measurements by Keene[9], and Ribe[10]. Later measurements than those of Fite et al. are also available, but since they confirm the results of Fite et al., they are not being represented here. The measurements of Fite et al. are about 20-25% larger compared to the the present, Dalgarno and Yadav, and Hunter and Kurian, results. Part of the discrepancy is due to the fact that in measurements, capture into the exited states of the projectile is included in the cross section, but not accounted in theory. This will be explained in the following figure.

Since capture into the excited states of the hydrogenic atoms at high energies decreases as $1/n^3$, Jackson and Schiff[11] have estimated that about 21% of the measured cross section is contribution of capture into the excited states. In Fig.2, based on this estimate, the experimental results are reduced by 21%, and as is seen good agreement is obtained between theories and measurements, falling the discrepancies within the experimental errors. In the right-hand-side ordinate of Fig. 2, instead of reducing the experimental results, we have increased the calculated results by a factor of 21%.

In Fig. 3 helium ion-helium atom charge exchange cross section is displayed. Our calculated results again are higher by 20-25% from those of Rapp and Francis[1]. More recent laboratory measurements of Helm[12], and Hegerberg, Stefansson and Elford[13] are also displayed . The measurement of Helm falls about 5% below our results at low energies, but at higher energies, the measurements of Hegerberg et al. fall almost on our calculated graphs. The agreement of our results with measurements is quite satisfactory. However, our calculation are not corrected for capture into the exited states.

To test the linearity of the plot of the squared root of the cross section versus the logarithm of the projectile energy, in Fig. 4 such a plot is shown. As seen in the figure, at high energies there is an increase in the slope of the graph. At still higher energies, the slope goes through some additional variations. Reason for this variation was given before. Calculated results of Moiseiwitsch[14] are also shown in this figure. We agree within a few percent with the calculated results of this author. The older measurements of Keene[9], Dillon et al.[15], and Jones et al.[16] are also shown in this figure. Experimental results of Dillon et al. tend to agree more with the calculational results of Rapp and Francis[1].

In figure 5, our results for Ne^+-Ne charge exchange cross sections are compared with the calculated results of Rapp and Francis[1], and the experimental results of Dillon et al.[15], and Flaks et al.[17]. The experimental results tend to agree more with the results of Rapp and Francis[1].

In Fig. 6 the case for Ar^+-Ar charge exchange is considered. Displayed are our results and those of Rapp and Francis[1], and six sets of laboratory measurements. Chronologically, the experimental results are due to Dillon et al.[15], Flaks et al.[17], Jones et al.[16], Kushnir et al.[18], Helm[12], and Hegerberg et al.[13]. Results of Kushnir et al., Hegerberg et al., Flaks et al., and Jones et al., as well as the low energy results of Helm, are in good agreement with our results. Results of Dillon et al. fall somewhat between our results and those of Rapp and Francis.

We also have calculated the charge exchange cross sections for Kr^+-Kr and Xe^+-Xe. Results are given in Figures 7 and 8, together with the experimental results available. As seen in the figures, for the Kr^+-Kr case, the experimental results of Flaks et al.[17], and Kushnir et al.[18] seems to be the continuation of each other, falling almost on a straight line, but have different slopes compared to our results.

Outside of the hydrogenic and closed shell atoms, we also have applied the method to a non-hydrogenic atom. Due to its aeronomical importance, we have calculated the resonance charge exchange for O^+-O system. This is shown in Fig. 9. The agreement of our results with the measured cross sections of Stebbings et al.[20], and Lindsay et al.[21], are far from satisfactory.

According to the method presented in this paper, if two atoms have the same ionization potentials, their cross sections should be the same. Since the ionization potential of atomic oxygen is only 0.15% larger than the ionization potential of atomic hydrogen, their charge exchange cross sections by our method should be almost identical. This has been tested in Fig. 10. As is seen, the theoretical results lie between the experimental values of Fite et al.[8] for atomic hydrogen on one hand, and the measurements of Stebbings et al.[20] and Lindsay et al[21]. for atomic oxygen on the other. No correction has been made in this figure for capture into the excited states of the projectile, which is present in measurement but not accounted for in the theory.

In Fig. 11 calculated charge exchange cross section for He^{++} on He^{+}, together with the measurements of Shepherd and Dickinson[25] are displayed. Due to coulomb repulsion, the cross section for this system should be zero at zero incident energy. Since this repulsion is absent in our formula, our model does not agree with measurements at low energies. But for energies larger than 100 eV, the calculated results are by 10-15% smaller than the measured values.

We also have applied the method to calculate the charge exchange cross sections for the case of H_2^{+}-H_2 . Results are given in Fig. 12 with three sets of experimental results. We have no agreement either in shape nor magnitude with the experimental results. Experimental results are also not consistent with each other.

CONCLUSION

The simple model presented here based on the work of Bates et al.[4], which bases the dependence of the symmetric resonance charge exchange cross section on quantum mechanical energy difference between the symmetric and anti symmetric states of the system wave function, is quite satisfactory for intermediate energy region, Since in hydrogenic atoms the energy difference can be approximated by the ionization potential of the target atom, evaluation of the charge exchange cross section is reduced to a knowledge of the atomic ionization potential. Results obtained for hydrogenic and some closed shell atoms compare favorably in accuracy in the intermediate energy range with the more elaborate perturbed stationary states calculations, and agreement with measurements is comparable to the experimental uncertainty.

TABLE I. Charge Transfer Cross Section for Hydrogen Atom-Hydrogen Ion

in units of πa_0^2

E(eV)	V(cm/s)	b^* Range	Number of Samples	Present	Ref. 1	Ref. 6
0.1	4.38+5	6.0 - 8.0	23	65.1 ± 0.4	56	
1	1.38+6	4.5 - 6.0	16	50.8 ± 0.3	41	53.7
10	4.38+6	0.5 - 4.5	9	37.9 ± 0.2	32	40.7
100	1.38+7	0.0 - 2.0	10	26.6 ± 0.2	20	29.1
1000	4.38+7	0.0 - 0.5	5	17.5 ± 0.1	12	18.8
10000	1.38+8	0.0 - 0.4	8	9.37	5.1	9.8
100000	4.38+8	0.0 - 0.0	4	1.451		2.1

REFERENCES

1. D. Rapp and W. E. Francis, J. Chem. Phys. **37**, 2631 (1962).
2. L. Pauling and E. B. Wilson, Introduction to Quantum Mechanics, (McGraw-Hill, New York, 1935).
3. J. C. Slater, Quantum Theory of Molecules and Solids, Vol. 1 (McGraw-Hill, New York, 1963).
4. D. R. Bates, H. S. W. Massey, and A. L. Stewart, Proc. Roe. Soc. A, **216**, 437 (1953).
5. J. D. Jackson, Canad. J. Phys. **32**, 60 (1954).
6. A. Dalgarno and H. N. Yadav, Proc. Phys. Soc. **A66**, 173 (1953).
7. G. Hunter and M. Kurian, Proc. Roy. Soc. (London) **A353**, 575 (1977).
8. W. L. Fite, R. F. Stebbings, D. G. Hummer, and R. T. Brackmann, Phys. Rev. **119**, 663(1960).
9. J. P. Keene, Phil. Mag. **40**, 369 (1949).
10. F. L. Ribe, Phys. Rev. **83**, 1217 (1951).
11. J. D. Jackson and H. Schiff, Phys. Rev. **89**, 359 (1953).
12. H. Helm, J. Phys. B: Mol. Phys. **10**, 3683 (1977).
13. R. Hegerberg, T. Stefansson, and M. T. Elford, J. Phys. B: At. Mol. Phys. **11**, 133 (1978).
14. B. L. Moiseiwitsch, Proc. Phys. Soc. (London) **A69**, 653 (1956).
15. J. A. Dillon, Jr, W.F. Sheridan, H. D. Edwards, and S. N. Ghosh, J. Chem. Phys. **23**, 776 (1955).
16. P. R. Jones, F.P. Ziemba, H. A. Moses, and E. Everhart, Phys. Rev. **113**, 182 (1959).
17. I. P. Flaks, and E. S. Solov'ev, Soviet Phys.-Tech. Phys. **3**, 564 (1958).
18. R.. M. Kushnir, B. M. Palyukh, and L. A. Sena, Bull. Acad. Sci. USSR, Phys. Ser. **23**, 995 (1959).
19. S. N. Ghosh, and W. F. Sheridan, J. Chem. Phys. **26**, 480 (1957).
20. R. F. Stebbings, A. C. H. Smith, and H. Ehrhartdt, J. Geophys. Res. **69**, 2349 (1964).
21. B. G. Lindsay, D. R. Sieglaff, K. A. Smith, and R. F. Stebbings, J. Geophys. Res. **106**, 8197 (2001).
22. A. Dalgarno, Phil. Trans. Roy. Soc. A250, 426 (1958).
23. H. Knof, E. A. Mason, and J. T. Vanderslice, J. Chem. Phys. **40**, 3548 (1964).
24. J. R. Stallcop, H. Partridge, and E. Levin,, J. Chem. Phys. **95**, 6429 (1991).
25. J. T. Shepherd, and A. S. Dickinson, J. Phys.. B: At. Mol. Opt. Phys. **33**, 2219 (2000).
26. J. B. H. Stedeford, and J. B. Hasted, Proc. Roy. Soc. (London) **A227**, 466 (1955).

FIGURE CAPTIONS

Figure 1. The present calculated charge exchange cross section is compared with similar calculation by Dalgarno and Yadav[6], D&Y, Hunter and Kurian[7], Rapp and Francis[1], R&F, and Jackson and Schiff[11], J&S. The measurements are due to Fite et a.[8], FSHB, Keen[9], K, and Ribe[10], R.

Figure 2. To exclude contribution to the cross section due to capture into the excited states of the projectile, the measured cross sections have been reduced by a factor of 1.2, bringing the measurements closer to the theory. On the right hand side ordinate of the figure, the theoretical results have been raised by a factor of 1.2.

Figure 3. The present calculational results for cross sections and those of Rapp and Francis[1], R &F, are compared to the measurements of Helm[12], Hm, and Hegerburg et al.[13], HSE.

Figure 4. Similar to Fig. 3, but the squared-root of the cross section is plotted versus the logarithm of the energy. The calculated results are those of the Present, Moiseiwitsch[14], M, and Rapp and Francis[1], R&F. The measurements are due to Helm[12], Hm, Hegerburg[13], HSE, Dillon et al.[15], DSEG, Keene[9], K, and Jones et al.[16], JZME.

Figure 5. The present calculational resuts and those of Rapp and Francis[1], R&F, are compared with the measurements of Dillon et al.[15], DSEG, Flaks et al.[17], F&S, and Jones et al.[16], JZME.

Figure 6. The present calculational results and those of Rapp and Francis[1], R&F, are compared to the measurements of Helm[12], H, Kushnir et al.[18], KPS, Dillon et al.[15], DSEG, Flaks and Solov'ev[17], F&S, and Jones et al.[16], JZME.

Figure 7. The present calculational results and those of Rapp and Francis[1], R&F, are compared to the measurements of Kushnir et al.[18], KPS, Dillon et al.[15], DSEG, Ghosh and Sheridan[19], G&S, and Flaks and Solov'ev[17], F&S.

Figure 8. The present calculational results and those of Rapp and Francis[1], R&F, are compared to the measurements of Kushnir et al.[18], Ghosh and Sheridan[19], G&S, Dillon et al.[15], DESG, and Flaks and Solov'ev[17]. F&S.

Figure 9. Resonance charge exchange between O^+ and O. Calculational cross section displayed are due to the present calculation, and those of Dalgarno[22], D, Rapp and Francis[1], R&F, Knof et al.[23], KMV, and Stallkop et al.[24], S&P. Measurements are due to Stebbings et al.[20], SSE, and Lindsay et al.[21], LSSS.

Figure 10. The experimental results of Fite et al.[8]. FSHB, for H^+ on H, and Stebbings et al.[20], SSE, and Lindsay et al.[21], LSSS, for O^+ on O are displayed together with the present model of calculation. Theoretically, the curve Present should represent cross section for both species. The curves FSHB and SSE contain captures into the excited states of the projectile, not accounted for in the calculation.

Figure 11. The present calculated cross section is compared to the measurement of Shepherd and Dickinson[25], S&D.

Figure 12. The present calculated cross section is compared to the measurement of Ghosh and Sheridan[19], G&S, Dillon et al.[15], DSEG, and Stedford and Hasted[26], S.

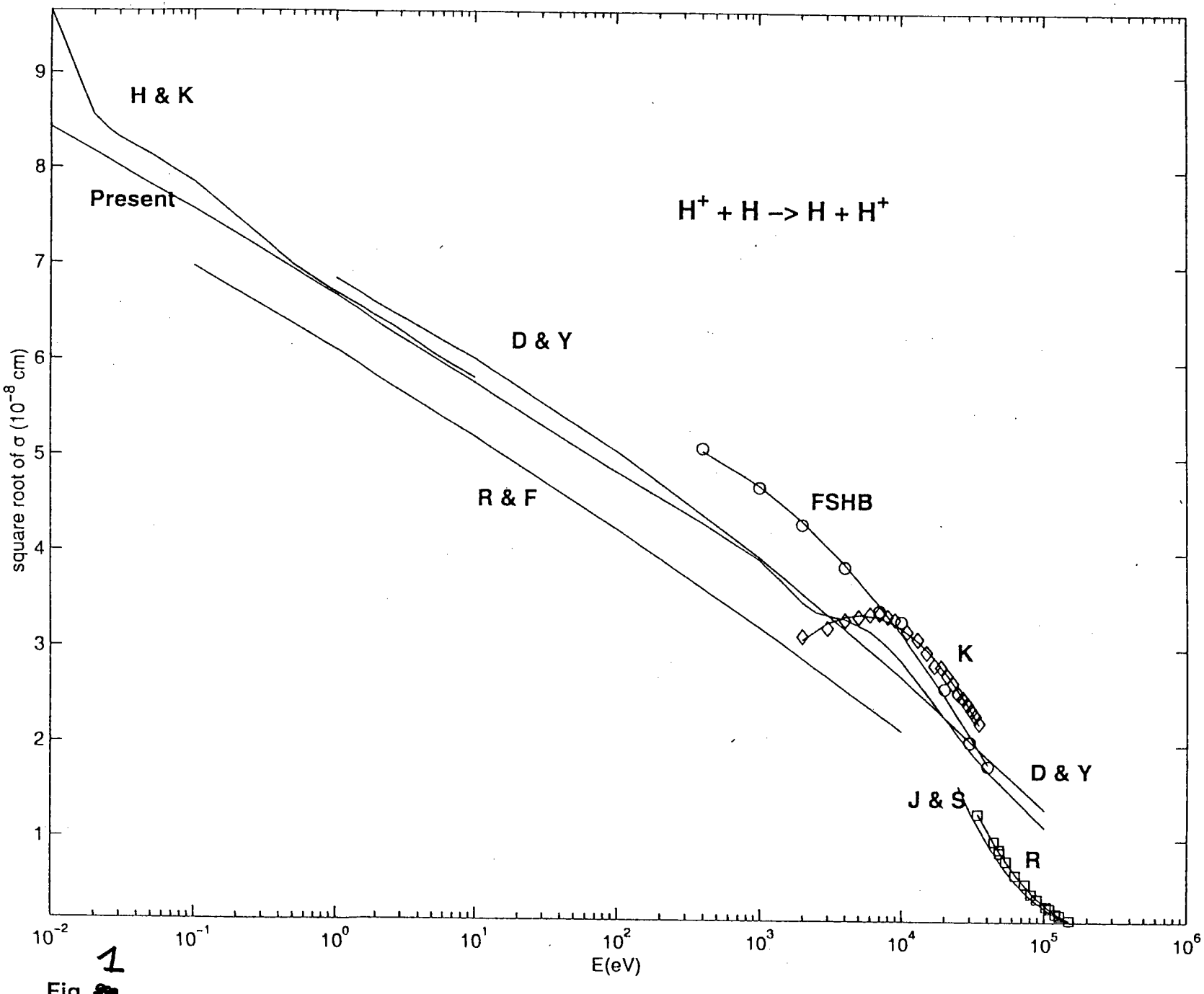
H & K
Present
D & Y
R & F
FSHB
K
D & Y
J & S
R
H+ + H -> H + H+
square root of σ (10-8 cm)
E(eV)
9
8
7
6
5
4
3
2
1
10-2
10-1
100
101
102
103
104
105
106

Fig. 1

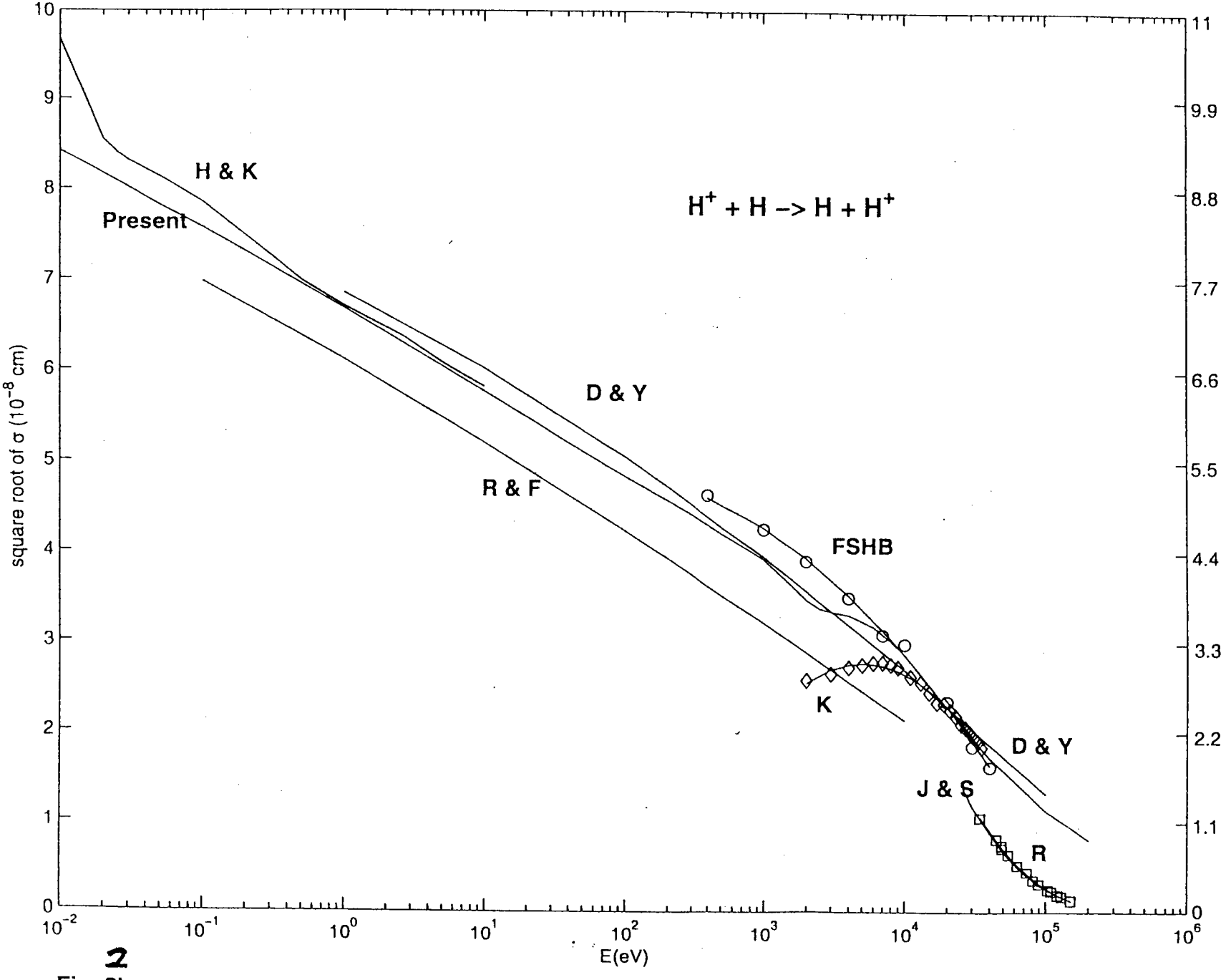
H & K
Present
$H^+ + H \rightarrow H + H^+$
D & Y
R & F
FSHB
K
D & Y
J & S
R
square root of σ (10^{-8} cm)
E(eV)

Fig. 2b

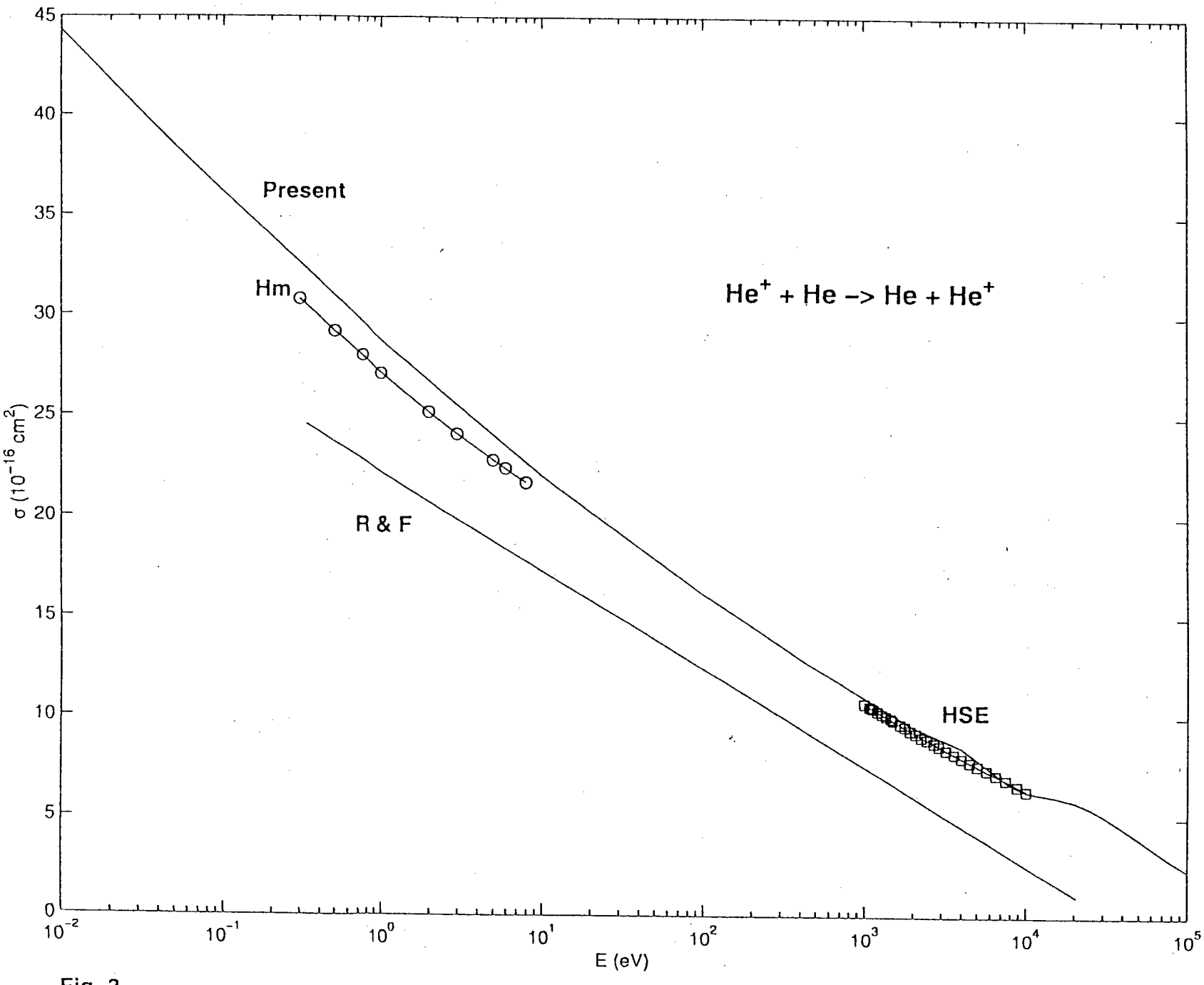
Present
Hm
R & F
HSE
$He^+ + He \rightarrow He + He^+$
$\sigma\ (10^{-16}\ cm^2)$
E (eV)
0
5
10
15
20
25
30
35
40
45
10^{-2}
10^{-1}
10^{0}
10^{1}
10^{2}
10^{3}
10^{4}
10^{5}

Fig. 3

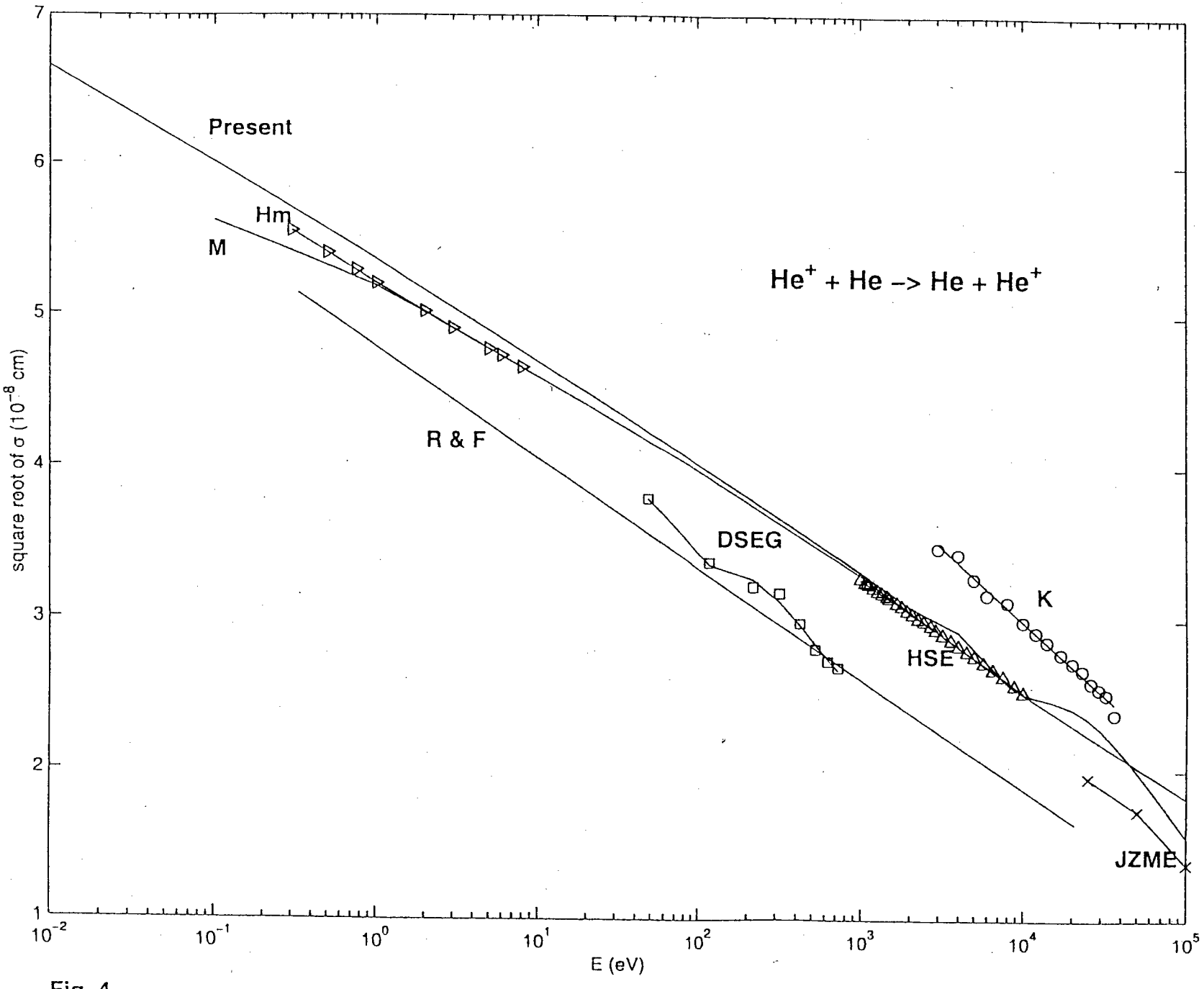
Present
Hm
M
R & F
DSEG
HSE
K
JZME
$He^+ + He \rightarrow He + He^+$
square root of σ (10^{-8} cm)
E (eV)
7
6
5
4
3
2
1
10^{-2}
10^{-1}
10^{0}
10^{1}
10^{2}
10^{3}
10^{4}
10^{5}

Fig. 4

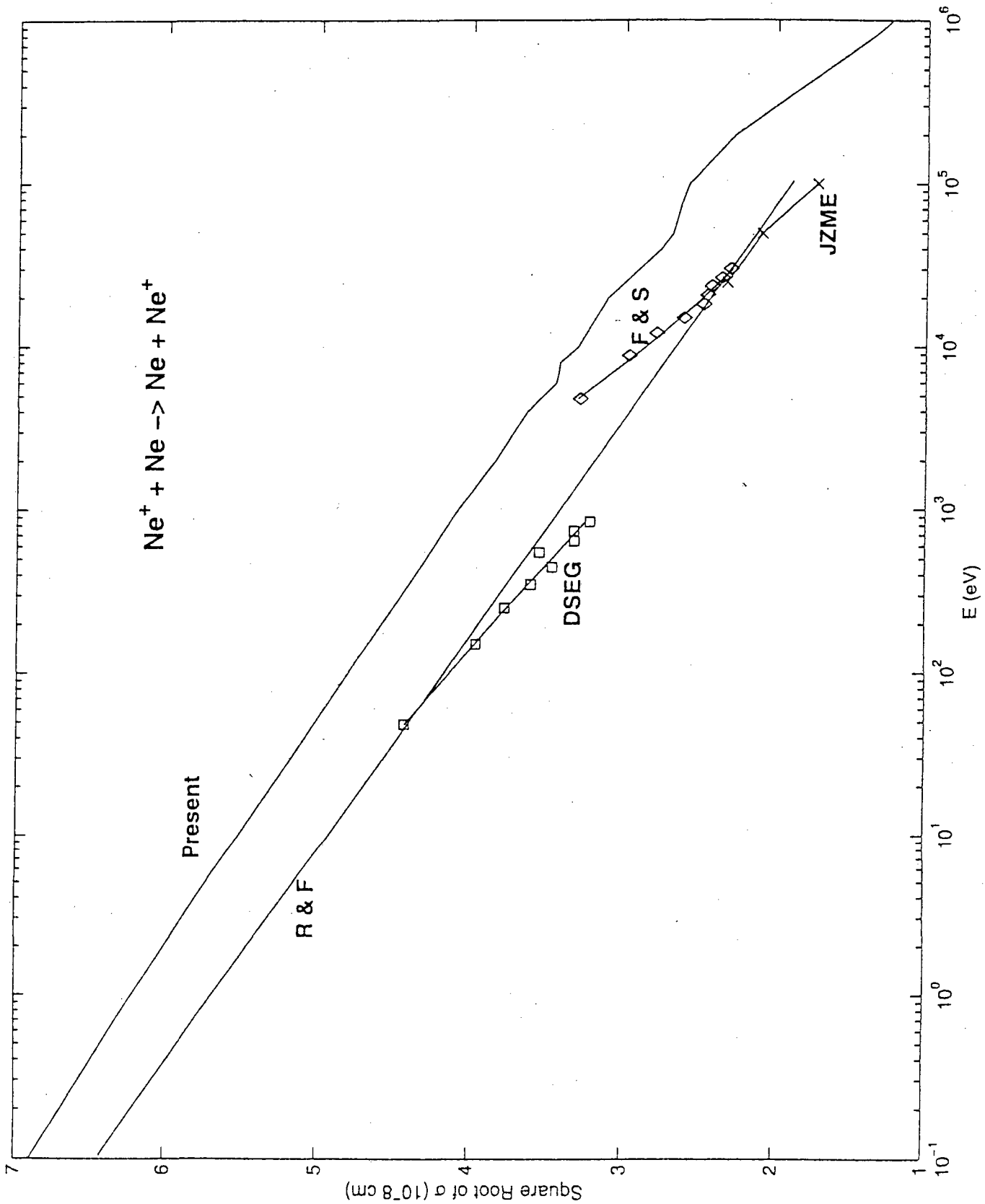
Ne+ + Ne –> Ne + Ne+
Present
R & F
DSEG
F & S
JZME
Square Root of σ (10^-8 cm)
E (eV)
1
2
3
4
5
6
7
10^-1
10^0
10^1
10^2
10^3
10^4
10^5
10^6

Fig. 5

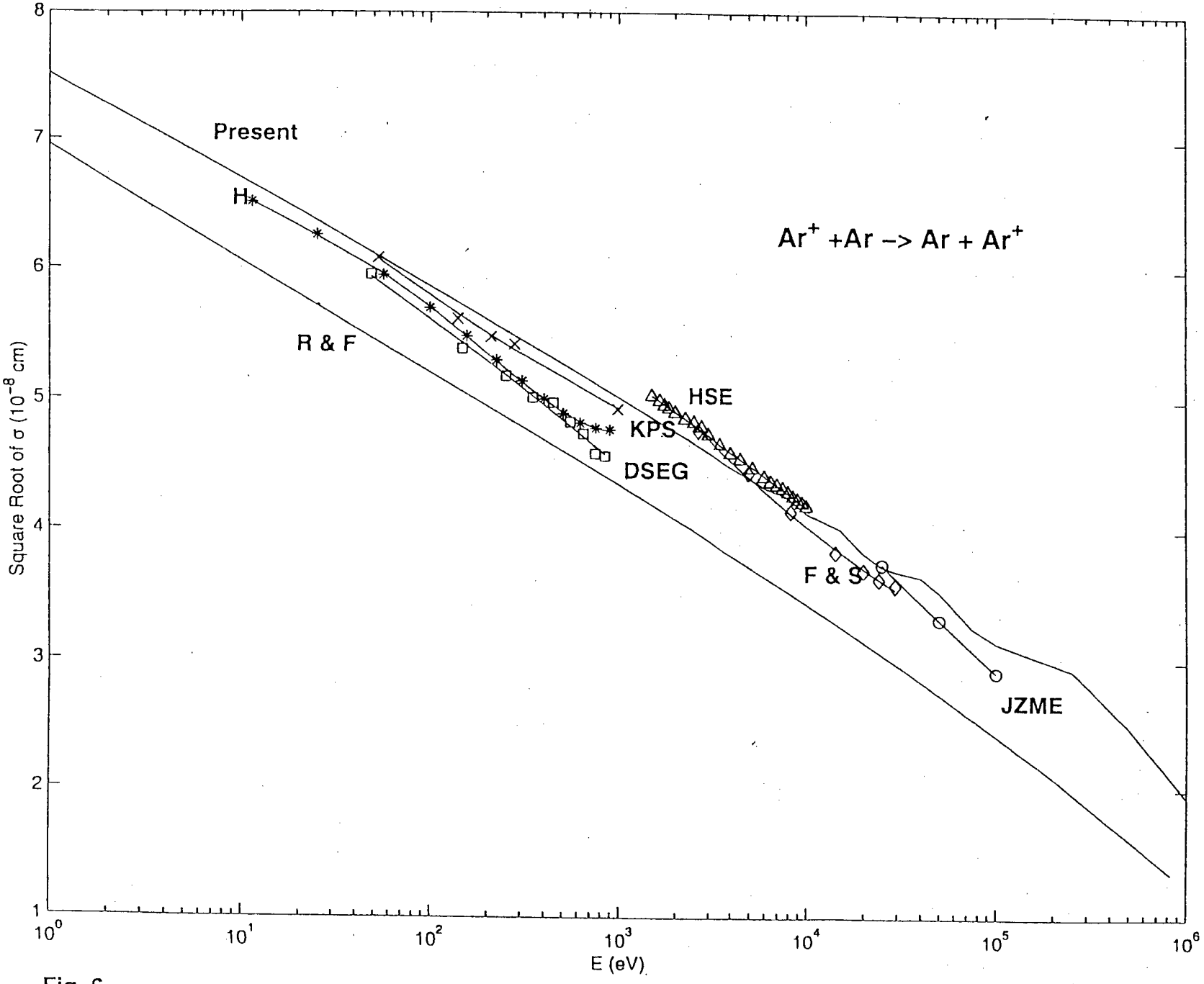
Present
H
R & F
HSE
KPS
DSEG
F & S
JZME
$Ar^+ + Ar \rightarrow Ar + Ar^+$
Square Root of σ (10^{-8} cm)
E (eV)
8
7
6
5
4
3
2
1
10^0
10^1
10^2
10^3
10^4
10^5
10^6

Fig. 6

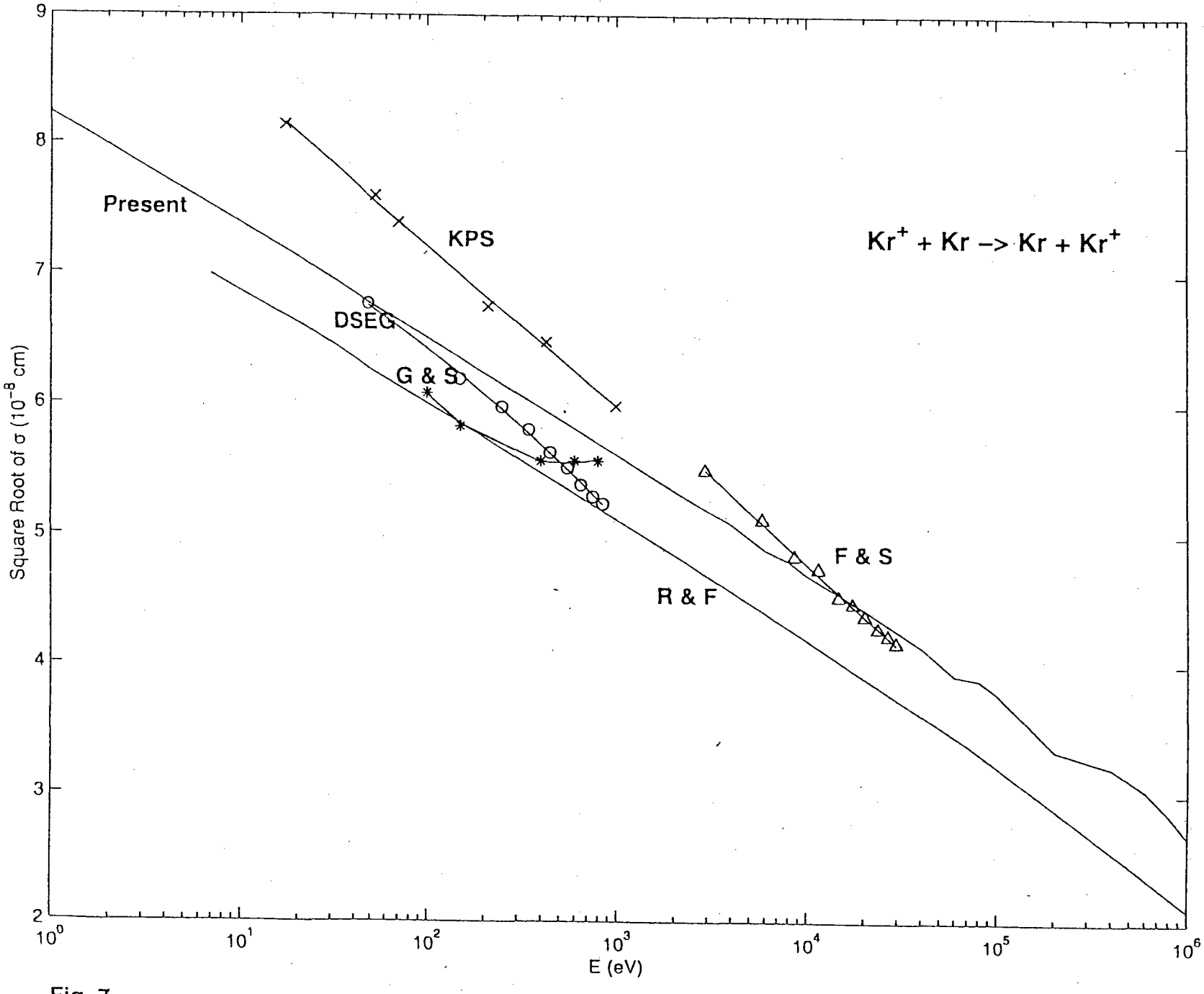
Present
KPS
DSEG
G & S
F & S
R & F
$Kr^+ + Kr \rightarrow Kr + Kr^+$
Square Root of σ (10^{-8} cm)
E (eV)
9
8
7
6
5
4
3
2
10^0
10^1
10^2
10^3
10^4
10^5
10^6

Fig. 7

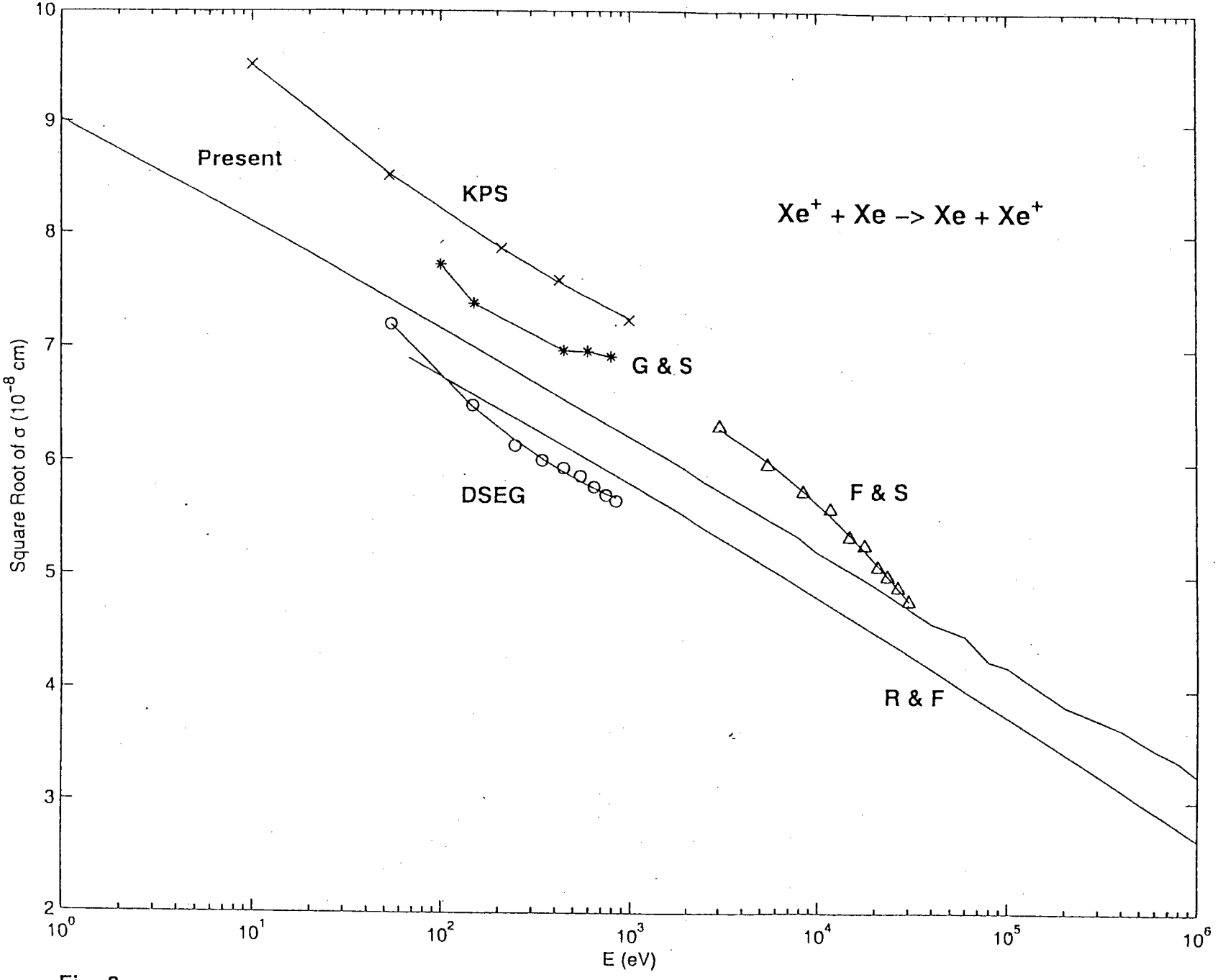
Present
KPS
G & S
DSEG
F & S
R & F
$Xe^+ + Xe \rightarrow Xe + Xe^+$
Square Root of σ (10^{-8} cm)
E (eV)
10
9
8
7
6
5
4
3
2
10^0
10^1
10^2
10^3
10^4
10^5
10^6

Fig. 8

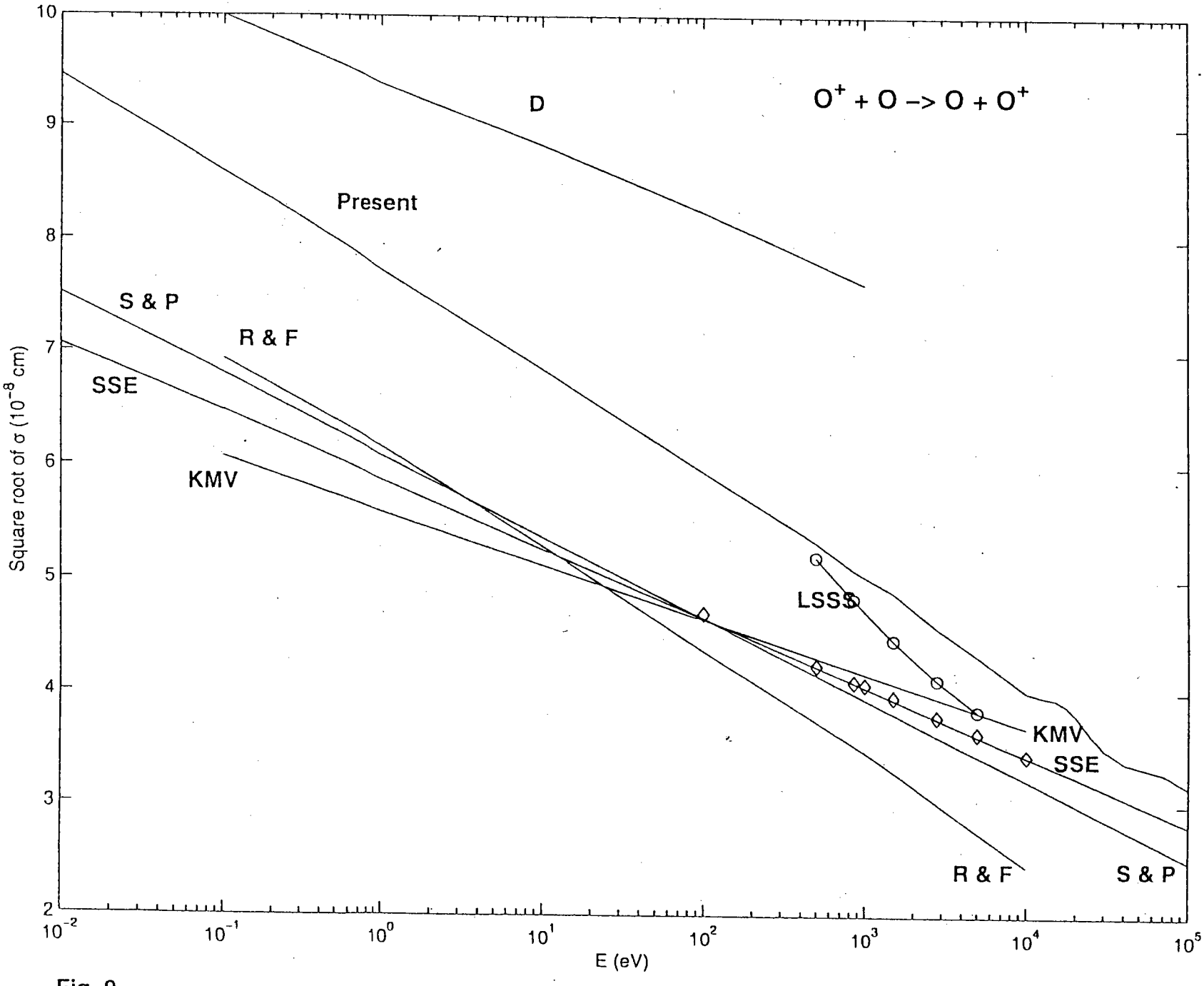
$O^+ + O \rightarrow O + O^+$
D
Present
S & P
R & F
SSE
KMV
LSSS
KMV
SSE
R & F
S & P
Square root of σ (10^{-8} cm)
E (eV)
10
9
8
7
6
5
4
3
2
10^{-2}
10^{-1}
10^{0}
10^{1}
10^{2}
10^{3}
10^{4}
10^{5}

Fig. 9

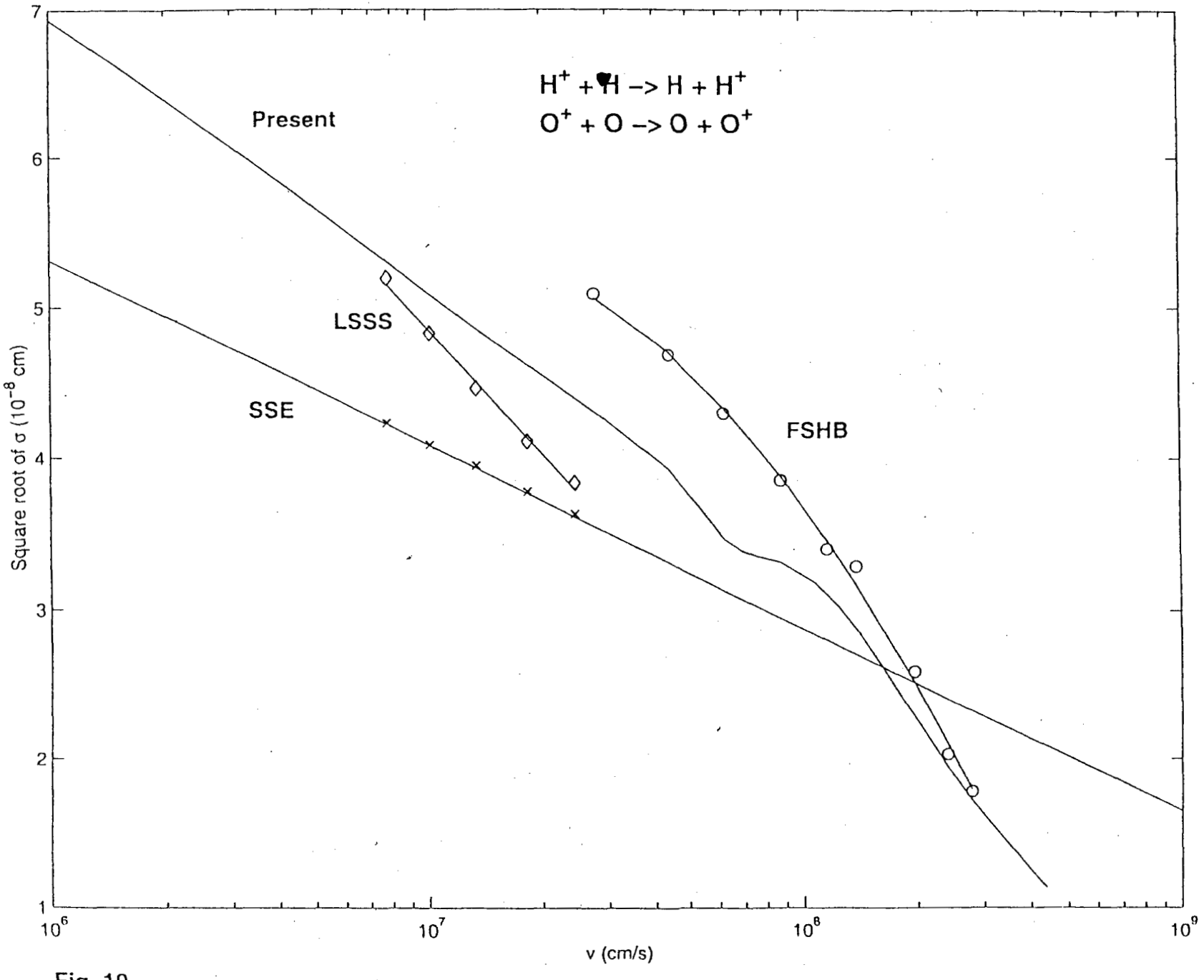
$H^+ + H \rightarrow H + H^+$
$O^+ + O \rightarrow O + O^+$
Present
LSSS
SSE
FSHB
Square root of σ (10^{-8} cm)
v (cm/s)
1
2
3
4
5
6
7
10^6
10^7
10^8
10^9

Fig. 10

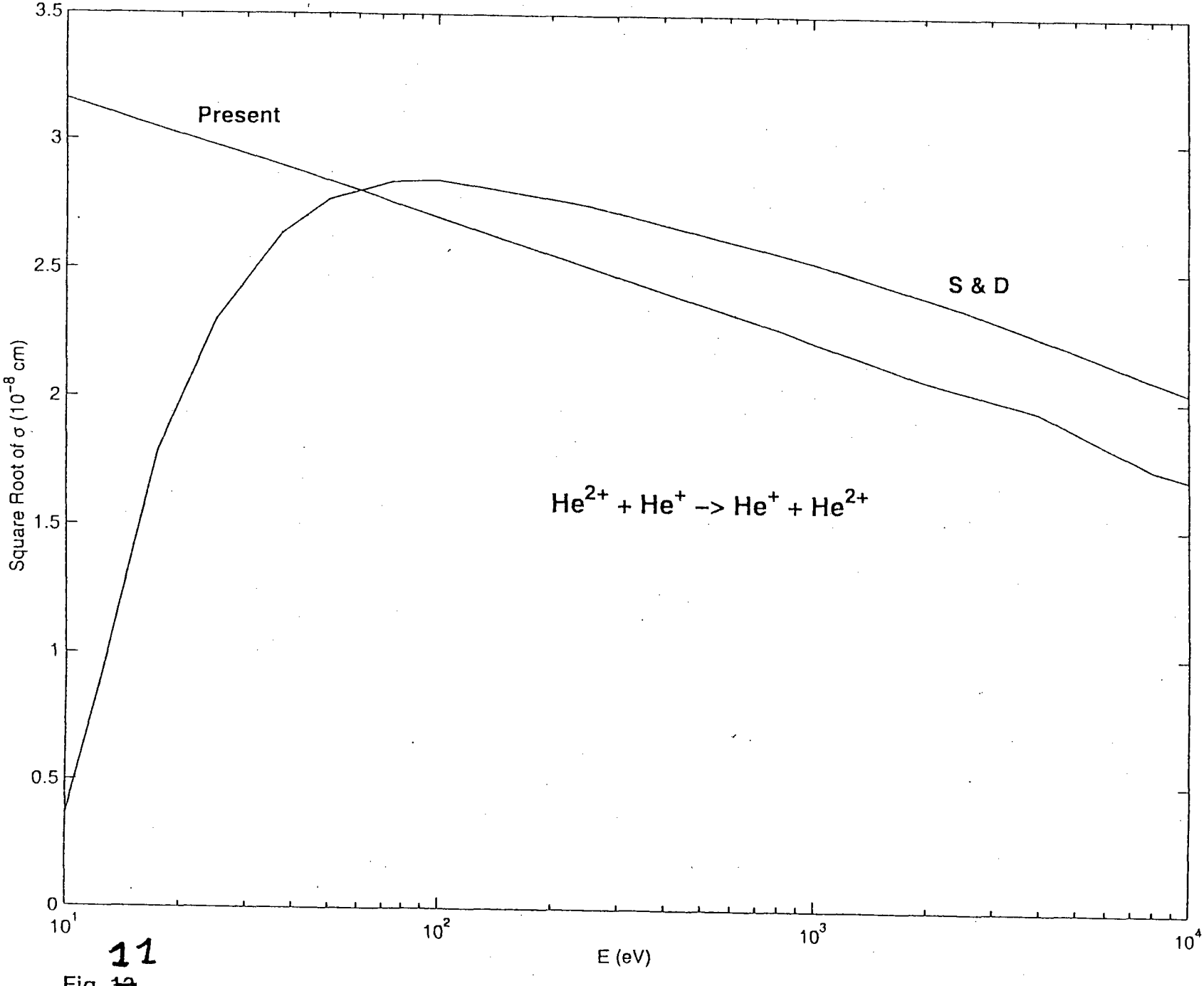
Present
S & D
$He^{2+} + He^{+} \rightarrow He^{+} + He^{2+}$
Square Root of σ (10^{-8} cm)
E (eV)
3.5
3
2.5
2
1.5
1
0.5
0
10^{1}
10^{2}
10^{3}
10^{4}

11

Fig. ~~12~~

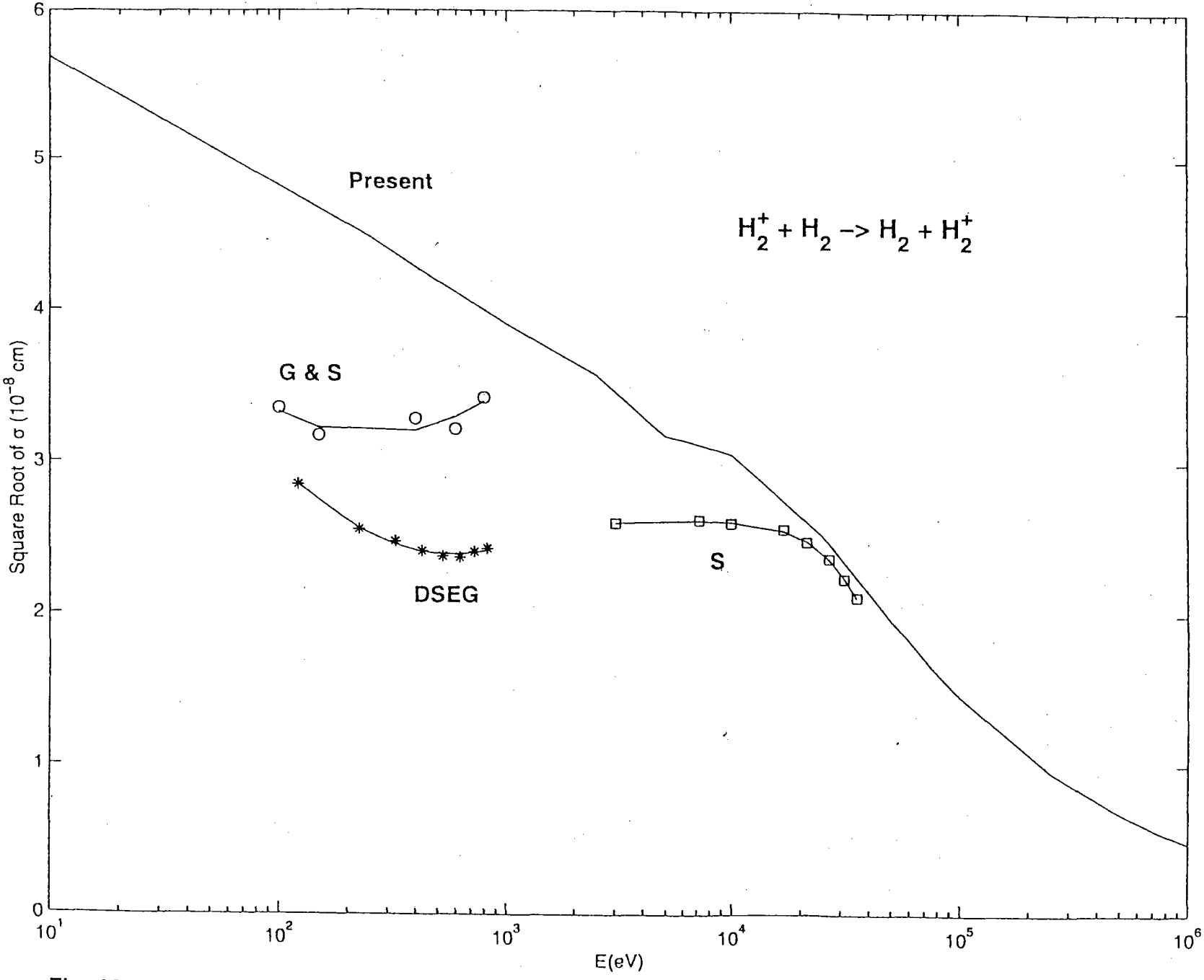
Present
$H_2^+ + H_2 \rightarrow H_2 + H_2^+$
G & S
DSEG
S
Square Root of σ (10^{-8} cm)
E(eV)
0
1
2
3
4
5
6
10^1
10^2
10^3
10^4
10^5
10^6

Fig. 12